Journal of Sustainable Construction Materials and Technologies
Web page info: https://jscmt.yildiz.edu.tr
DOI: 10.14744/jscmt.2021.06

JSCMT
Journal of Sustainable Construction Materials and Technologies

Review Article

Application of finite element method on recycled aggregate concrete and reinforced recycled aggregate concrete: A review

Hasan DİLBAS

Department of Civil Engineering, Van Yüzüncü Yıl University, Engineering Faculty, Van, Turkey

ARTICLE INFO

Article history
Received: 18 November 2021
Accepted: 11 December 2021

Key words:
Dynamic loading, finite element, recycled aggregate concrete, reinforced recycled aggregate concrete, static loading

ABSTRACT

In recent years, concrete has become a widely used material for general purposes in the structural area due to its excellent performance and properties. Hence, an increasing number of concrete structures are built, and a huge amount of building stock has been occurred around the world. However, because of the many progress (i.e., natural disasters), some of the concrete structures are demolished and their status is changed into rubble, and hence this becomes an environmental problem threatening the nature. To struggle with the rubbles, – a brilliant idea – recycling concrete is appeared and to disposal the rubbles in concrete works become a subject in the authorities' agenda. Also, according to the brilliant approach, the studies focus on some experiments and simulation works (i.e., finite element modeling) to analyze the use of rubbles as recycled aggregate (RA) in concrete, recycled aggregate concrete (RAC) and reinforced RAC (RRAC) properties. At this point when a deep look is concentrated on the papers on RAC and RRAC, the reviews generally include experimental works of the research but rarely or hardly ever consider the simulation stages of the researche. Hence, this paper is drawn as a state-of-the-art report on modeling works of RAC and RRAC. Also, this paper gives finite element model (FEM) details of the examined research to improve the future studies on RAC and RRAC with helpful comments and directions.

Cite this article as: Dilbas H. Application of finite element method on recycled aggregate concrete and reinforced recycled aggregate concrete: A review. J Sustain Const Mater Technol 2021;6:4:173–191.

1. INTRODUCTION

Concrete, in present, is widely used due to its excellent structural performance with rebars, strong resistive behavior to harmful environment, low-cost requirements for the maintenance and plastic behavior in fresh state, and a huge amount of structure have been built in the world. Hence, the stock of the reinforced concrete structures has been increased with the urbanization moves of the countries. As a results of the natural disasters, the change in the human demands, and the urban renewal plans etc. many engineering structures have been demolished and their status have been turned into waste [1]. In this situation, it caused million tons of construction and demolished waste (C&DW) in the world [2]. To struggle with C&DW, many countries have taken positions and made new regulations, taken out

*Corresponding author.
*E-mail address: hasandilbas@yyu.edu.tr

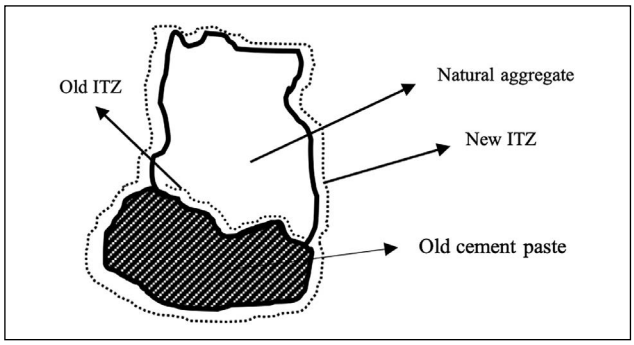

Figure 1. The structure of RA.

new laws, and revamped the current urban plans etc. [3, 4]. On the other hand, a huge amount of C&DW and its potential use in concrete as an aggregate (recycled aggregate (RA) inspire the researchers to conduct comprehensive studies. Hence, fully, or partially use of RA is considered in the studies and the effect of RA and other components (i.e., mineral admixtures) widely examined (i.e., [2, 4–8]). The physical and the mechanical properties, and the durability properties of recycled aggregate concrete (RAC) are mainly discussed and valuable comments/recommendations on RAC are stated in the literature [2, 4–8]. For instance, the optimum RA use ratio is mostly suggested by many researchers as 30% in concrete mixtures [2, 5].

On behalf of the studies on RA, it can be said that RA has mainly two parts: Natural aggregate (NA) and adhered old cement paste (OCP). Additionally, interfacial transition zone (ITZ) between NA and OCP can be considered as a part of RA. When the properties of RA are considered, the poor property of RA is usually sourced by OCP which has lower elasticity modulus, lower strength, and more porous structure than NA [2]. On the other hand, if RA is considered to utilize in concrete mixtures, four main things occur (Fig. 1): NA, OCP, new ITZ and old ITZ [2]. Also, SEM observations of RAC in Figure 2 is precisely demonstrated the structure of RA. It can be seen in Figure 2 that there are many cracks and voids between the RA and mortar matrix and it is clear that the components of RA negatively affect the properties of RA and so RAC [2].

In present, the properties of RAC and RRAC can be determined with various instruments using many techniques. As above mentioned, SEM is one of the instruments and it depends on experiments and, mechanical tests (compressive, tensile, etc.) are some the other instruments used in the literature widely. In this perspective, it is well-known that it is possible to estimate the concrete or the reinforced concrete behaviors with simulation models if the model is composed properly. The finite element method is widely used method in modeling research in the literature, and the finite element analysis (FEA) gives consistent results with experiments is proven in many conducted research (i.e., [9–11]).

When a deep look is concentrated on the related literature, the research on RA is usually conducted in two parts: an experimental stage and a modeling stage (i.e., [12–18]). In the research, after or before the experiments, a modeling stage is usually examined, and the theoretical results obtained from modeling part are verified with the experimental results. The results are generally used to show that FE model (FEM) is suitable to estimate the behavior of concrete under various conditions (i.e., static loading). Hence, FEA takes part in the studies and has an importance as much as experiments have; and perhaps the most important thing is that the verified models can supply additional data without conducting any additional experiments to estimate the concrete behavior.

However, when someone sets eye on the review works on RAC and RRAC, the reviews generally report experimental parts and rarely or hardly ever consider the simulation stages of the research (i.e., [2, 13–15]). Hence, to fill the gap in the literature and to summarize the research included finite element (FE) modeling works, this paper is not only drawn primarily as a state-of-the-art report on modeling of RAC, but also written as a state-of-art on mod-

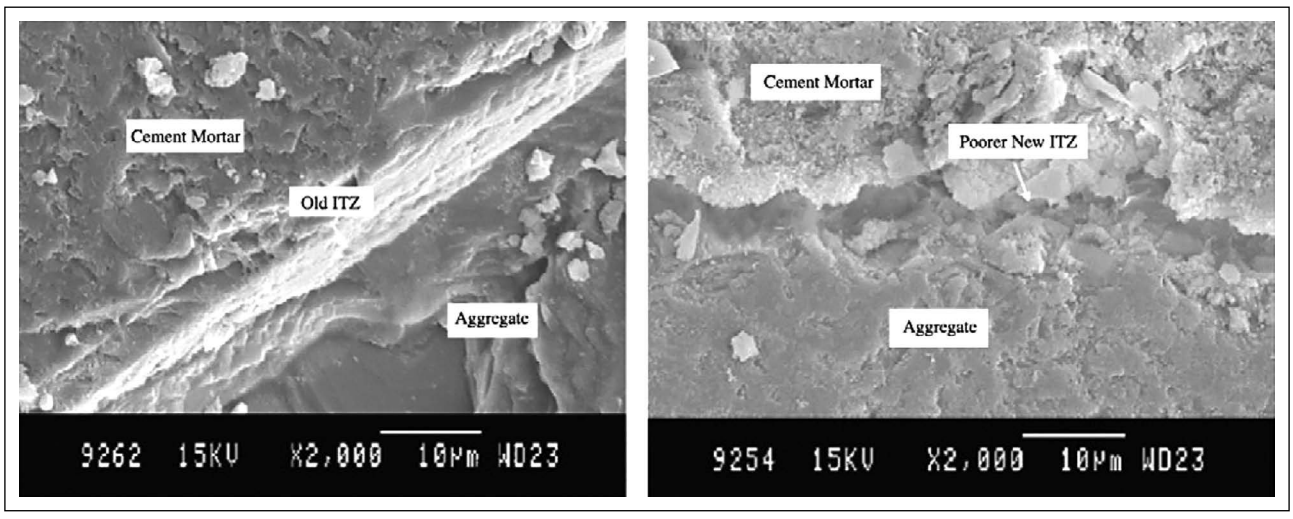

Figure 2. The microstructure characteristics of RAC [2].

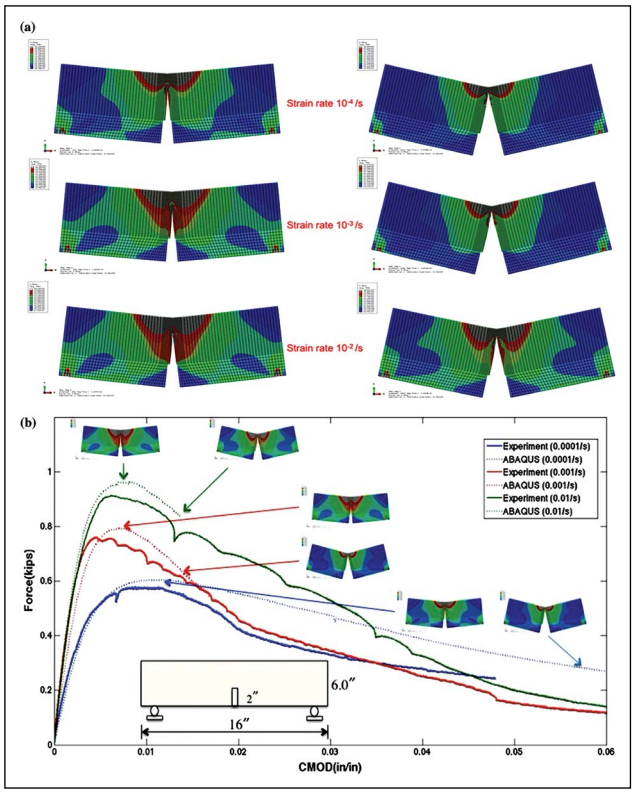

Figure 3. Force versus CMOD and stress distributions for Case 1: fixed beam size under three different loading rates, stress distribution at peak loads and final deformed stages for Case 1, Full force versus CMOD curves for Case 1 [23].

eling of RRAC. In addition, this review gives the details of FEMs of the related research to improve the future studies on RAC and RRAC with helpful comments and directions.

2. RECYCLED AGGREGATE CONCRETE

It is well-known that RAC has poor properties (low strength [5, 19], low elasticity modulus [19], etc.) in comparison to conventional concrete (NAC)due to its components, and the low properties of RAC usually sourced by RA [20]. RA has lower strength, elasticity modulus and porous structure with cracks [13] and ITZ is a crucial component in RAC [5]. Hence, the works on RAC generally concentrate on modeling ITZ and RA in macro-, meso- and micro-scales. In this perspective, the related research is examined in three subsections as given in below.

2.1. Modeling of Recycled Aggregate Concrete

2.1.1. Macro-Scale Modeling

In the literature, researchers examine the macro-scale behavior of RAC in pure concrete state and in confined concrete state (concrete filled steel tube (CFST)). Hence, in this review paper, the subject of "Modeling of Recycled Aggregate Concrete" is divided into two parts as one can see in below considering the details given above.

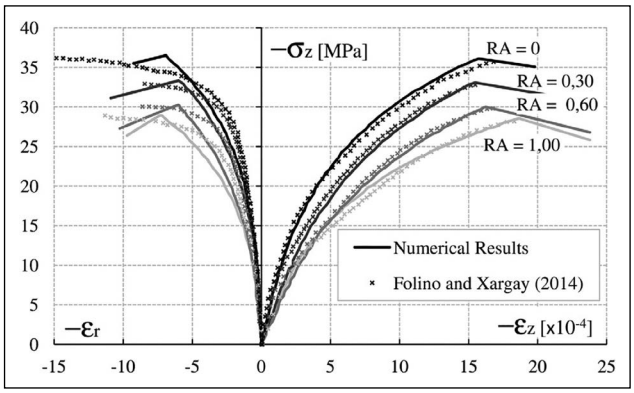

Figure 4. Numerical results of uniaxial compression tests against experimental results by Folino and Xargay [24].

2.1.1.1. Macro-Scale Behavior of RAC in Pure RAC State

Etse et al. [21] improve a constitutive theory for RAC considering high temperature conditions. The theory is a material model of thermodynamically consistent gradient poroplastic and aims to predict the mechanical behavior of RAC [21]. In the research, the elevated temperatures (20-200-400-600°C) and various RA ratios (0-30-60-100%) are concerned and the RAC simulation of the failure behavior under high temperature and the capability of the theory are demonstrated [21].

Dilbas [4], in his research, conducts some mechanical tests (compressive strength, splitting tensile strength and elasticity modulus) to define the mechanical behavior of RAC obtaining stress-strain data from zero to failure and beyond for mechanical tests [4]. Then, a homogeneous cantilever beam subjected to a point load is modeled in his research using the obtained mechanical properties and the mechanical behavior is examined under static loading conditions in Abaqus [4]. In his research, 3-dimensional (3D) non-linear FEA is considered, and pure plasticity is used to define the RAC properties in Abaqus [4]. Also, the results are verified with SAP 2000 FEA software.

Choubey et al. [22] demonstrate the application of fracture models to RAC (double-K fracture model and fictitious crack model). The required parameters for the models are obtained in the equations given in the related literature and varying content of RA (0-30-50-70-100%) is considered [22]. It is concluded that the fracture models given in the literature for natural aggregate concrete (NAC) is suitable for RAC and the fracture parameters of RAC included RA from 0% to 100% can be determined using the models [22]. Also, some interesting results for NAC and RAC are found that the ratio of Pini/Pu (force when initial crack occurs/ultimate force) and KICini/KICun (initial cracking toughness/unstable fracture toughness) are constant for RAC and NAC [22].

Musiket et al. [23] present the fracture tests on notched RAC beams with different sizes under different high loading rates from 10−4/s to 10−2/s (Fig. 3) considering and combining two material models: viscoelastic model and

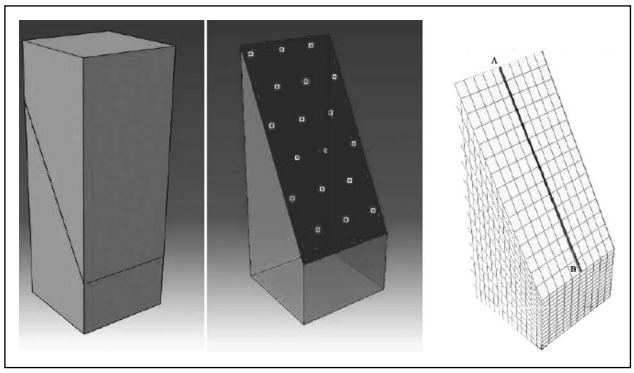

Figure 5. Parts assembled (left), surface definition (right) and mean line of the interface [25].

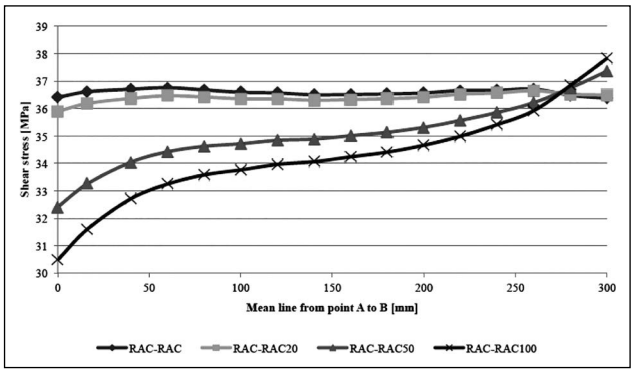

Figure 6. Evaluation of the shear stress in the interface [25].

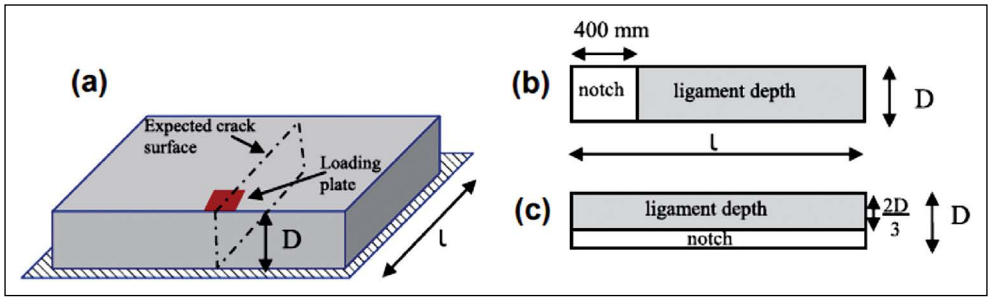

Figure 7. **(a)** Slab specimen on soil with expected crack surface; **(b)** edge-notched slab; and **(c)** one-third notched slab. Gray area in **(b and c)** denotes the ligament, while the white area is the pre-existing notch [9].

multi-phase composite model. Combining two material models, the rigidity of RAC is predicted for high loading rate conditions [23]. Force-crack mouth opening displacement (CMOD) curves are obtained from simulations, and the simulation model includes the fracture analysis criteria and eXtended Finite Element Method (XFEM) [23]. As a results, similar distributions of stress in the beams for different sizes are obtained, and the maximum loads estimated by the simulations are not close with test data [23].

Ripani et al. [24] study on a gradient plasticity theory reformulating Leon-Druger-Prager Model. The theory is widened to estimate the mechanical failure behavior of RAC, and the supposed theory is consistent with thermodynamic laws and considers the softening and hardening response behaviors [24]. In the modeling section, the supposed model and some numerical results are compared against experimental results given in the literature and the formulation of dual mixed FE is considered [24]. The formulation includes thermodynamically consistent gradient plasticity [24]. Also, the tests of uniaxial tensile and compression are adopted to FEM [24]. It is stated in conclusion that the proposed constitutive model presents the influence of RA addition on the behavior of failure response and reflects the sensitivity of RA [24] (Fig. 4).

Ceia [25] researches the effect of RA on shear resistance. In the experimental work, many specimens including various RA ratios (0-20-50-100%) are produced [25]. In the 3D modeling section, Abaqus is used, two parts (upper and lower parts) are defined separately to model the shear test and then the parts are assembled in conformity with a behavior of linear elastic material [25] (Fig. 5). Cohesive bonding is considered for the surfaces of the specimens [25]. It is stated that the stiffness of differential in FEA is substantial for shear strength [25] (Fig. 6).

Gaedicke et al. [9] propose an 3D approach which includes three subjects separately: Concrete slab flexural load capacity determination under mode I -the slab lies on elastic foundation-, crack growth and crack initiation. 3D slabs FEM is generated in Abaqus, and the slabs include cohesive crack elements along pre-defined paths [9] (Fig. 7). The bilinear softening for concrete is considered, and the model is simulated. Also, the results are verified experimentally [9]. It is concluded that 3D cohesive crack element can estimate the capacity of slabs under flexural loads on soils [9].

2.1.1.2. Macro-Scale Behavior of RAC in Confined RAC State

Tam et al. [26] use RAC in concrete-filled steel tubular (CFST) columns as a filling material and CFST columns has rectangular geometry. Then FEA is considered to model CFST columns in Abaqus [26]. An equation defined for stress-strain data for confined concrete proposed by Han et al. [26] is used in the model as a constitutive model parameter and it is stated that the equation gives good results for models when the damage plasticity model is used in Ab-

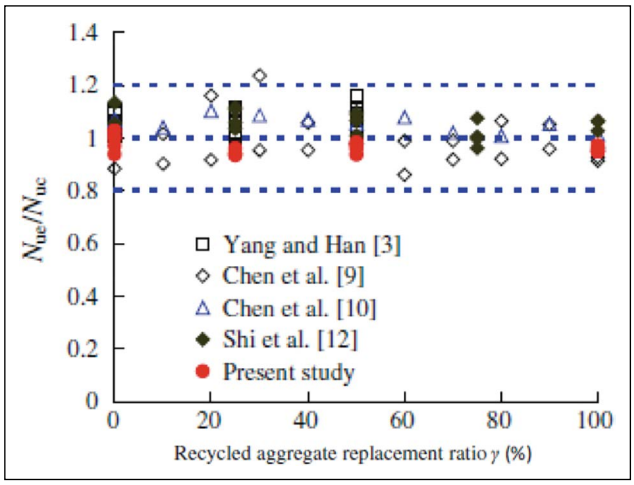

Figure 8. Comparison between the predicted and experimental ultimate strength [26].

aqus [26]. In the modeling part, steel jacket and concrete are modeled as shell and solid elements, respectively [26]. Also, surface-based interaction between the steel jacket and concrete is defined: In the normal direction and the tangential direction a contact pressure model and a Coulomb friction model, respectively [26]. In conclusion, it is stated that a FE model simulated for conventional concrete-filled steel tubes is possible to use for CFST with RAC, and satisfactory CFST results are found [26] (Fig. 8).

Yang et al. [27] carry out an experimental and numerical studies on square CFST under lateral impact loads (Fig. 9). In this study, local damages and failure modes of specimens are examined [27]. The non-linear FEM for CFST is simulated in Abaqus, and explicit solver is considered. [27]. Damaged plasticity model is taken into account for modeling nonlinear behavior of concrete [27]. It is found that the failure mode of CFST is generally concave where the loads are applied to, and the shear failure with punching shear failure of CFST is observed [27]. Also, experimental, and numerical results are in good agreements is found [27].

Xiao et al. [28] use glass fiber reinforced plastic (GFRP) tubes and steel tubes to confine RAC in their research and apply axial compression force to concrete-filled tubes to determine the mechanical properties. Then, a concrete-filled tube FEM is simulated to examine the outer tube thickness and the core strength effect [28]. The non-linearity in FEM is accounted in ANSYS [28]. 3D solid element for outer tube is used and the element abilities are creep, plasticity, stress stiffening, swelling, large strain, and large deflection, and the name is solid45 [28]. Also, 3D solid element for core concrete is chosen and the name is solid65 [28]. Solid65 is for solid models including no rebars and the abilities of solid65 are crushing in compression, cracking, creep cracking in tension and plastic deformation [28]. It is concluded that the peak stress of recycled concrete filled steel tube increases when the thickness increases and no effect on the plastic stage is observed [28] (Fig. 10).

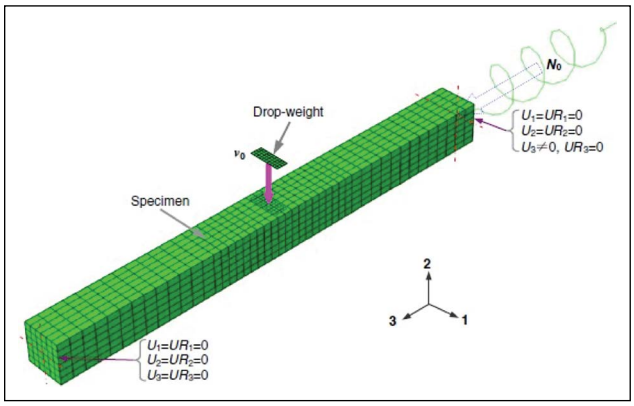

Figure 9. A schematic view of the test assembly [27].

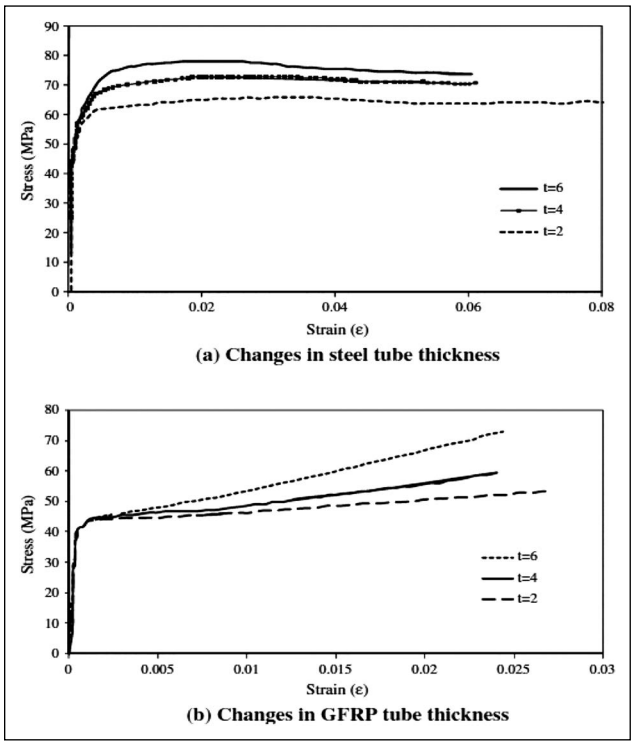

Figure 10. Effect of the outer tube thickness [28].

Xiang et al. [29] conduct a theoretical study on recycled aggregate concrete-filled steel tube stub columns. In the study, cold-formed hollow structural square steel tube is used, and nonlinear finite element model is simulated in Abaqus [29]. The stub column is subjected to axial compression. 3D eight-node solid elements with full integration (C3D8) are chosen for rigid plates and RAC, and the cold-formed steel tube is modeled with a shell element (S4) due to the small wall thickness in Abaqus [29]. For modeling the cold-formed steel material behavior, an idealized elastic-plastic stress-strain model proposed by Abdel-Rahman and Sivakumaran is considered [29]. This model indicates a multi-linear isotropic strain hardening rule [29]. The ascending part of RAC equivalent stress-strain is modeled according to Guo and Zhang equation [29]. Concrete damaged plasticity model in Abaqus

Table 1. Comparisons of the ultimate compressive strengths determined by different methods [29]

Specimen	Eurocode 4		ACI 318-05		ANSI/AISC 360-05		Sakino		Han	
	P_{EC4}(kN)	P_{EC4} / P_{TEST}	P_{ACI} (kN)	P_{ACI} / P_{TEST}	P_{AISC} (kN)	P_{AISC} / P_{TEST}	P_{Sakino} (kN)	P_{Sakino} / P_{TEST}	P_{Han} (kN)	P_{Han} / P_{TEST}
Sa1-1	610	0.946	563	0.873	559	0.867	605	0.938	598	0.927
Sa1-2	610	0.924	563	0.853	559	0.847	605	0.917	598	0.906
Sa2-1	567	0.909	526	0.843	523	0.838	559	0.896	557	0.893
Sa2-2	567	0.923	526	0.857	523	0.852	559	0.910	557	0.907
Sb1-1	1305	1.020	1197	0.936	1191	0.931	1290	1.009	1283	1.003
Sb1-2	1305	1.014	1197	0.930	1191	0.925	1290	1.002	1283	0.997
Sb2-1	1207	0.966	1114	0.890	1108	0.886	1192	0.954	1191	0.953
Sb2-2	1207	0.933	1114	0.861	1108	0.857	1192	0.922	1191	0.921
Sc1-1	2230	1.050	2038	0.960	2027	0.955	2147	1.011	2191	1.032
Sc1-2	2230	0.996	2038	0.911	2027	0.906	2147	0.959	2191	0.979
Sc2-1	2055	0.980	1889	0.900	1880	0.896	1979	0.943	2026	0.966
Sc2-2	2055	0.960	1889	0.883	1880	0.879	1979	0.925	2026	0.947
Mean		0.968		0.891		0.887		0.949		0.953
COV		0.044		0.040		0.040		0.040		0.044

is considered for RAC, and the surface-to-surface contact is used for the relation between the faces of steel jacket and core concrete [29]. In the research section on the friction coefficient, it is stated that the column under compression has no sensitivity with the friction coefficients although various friction coefficients (from 0.2 to 0.6) in FEM is considered [29]. In conclusion it is stated that the square CFST included RAC has similar mechanical behavior with the square CFST included conventional concrete, and the specification Eurocode 4 estimates the ultimate compressive strength of square CFST with a reasonable accuracy [29] (Table 1).

Yang et al. [30] investigate the fire resistance of CFST included RAC (Fig. 11). In the analysis, typical temperature development, failure pattern, fire resistance and axial displacement of the specimens are determined [30]. In the simulation, RAC-filled square steel tubular columns is modeled in Abaqus [30]. According to the research, the model includes two main parts: thermal part (includes temperature development) and mechanical part (includes displacement, failure pattern, and fire resistance) [30]. In the model, the effects of radiation and heat convection on column is taken into account [30]. The thermal contact resistance between the core RAC and steel tube is considered in conformity of the suggestion of Ghojel [30]. In the heat transfer model, the core concrete and the steel jacket are modeled with linear 3D brick elements (DC3D8) and 3D shell elements (DS4), respectively [30]. Under high temperatures, plasticity model is used for steel tubes and the damaged plasticity model for core concrete is adopted [30]. The 'Coulomb friction' and 'hard contact' is chosen for the contact properties between core and steel, and geometric linearity is assumed for large lateral deflections [30]. In conclusion, it is stated that the temperature development and fire resistance, failure pattern and axial displacement of specimens with 50% RA are generally similar behavior with reference CFST, and the estimated response of CFST under fire is generally in good agreement with experiments [30].

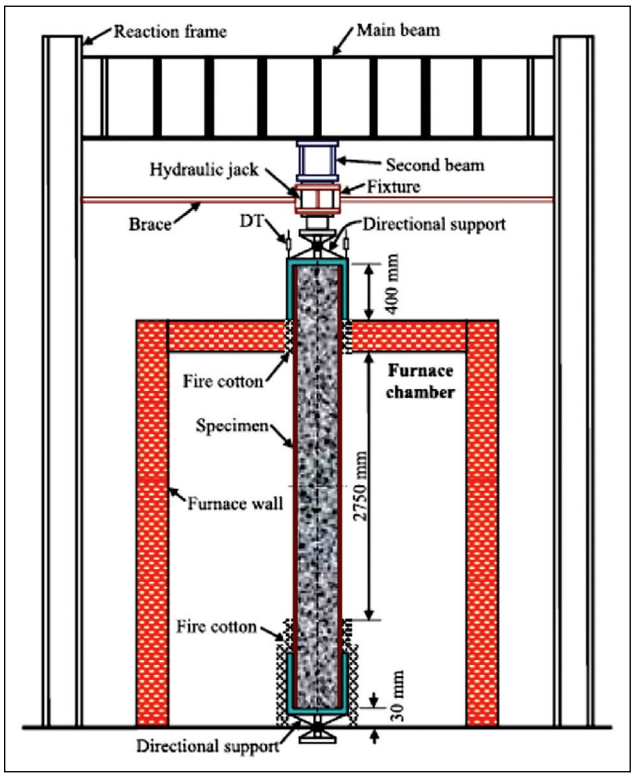

Figure 11. Schematic diagram of the test set-up [30].

Geng et al. [31] examine the time-dependent behavior of CFST with RAC (50 MPa). In this paper, a CFST is modeled in Abaqus. Core concrete and steel tubes are considered in Abaqus as Timoshenko beam elements (B31) and the time-dependent behavior of concrete is formed considering the Fathifazl creep model [31]. Under compression, the concrete constitutive model in Abaqus with the UMAT subroutine is used [31]. As a results, FEM gives a good agreement with the numerical results and the FEA results with the maximum deviation 1.9‰ is obtained in comparison to the numerical results [31].

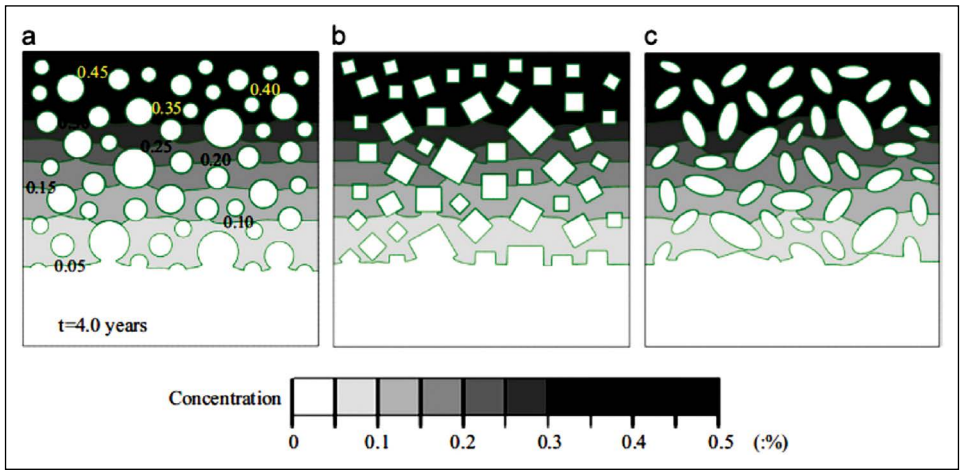

Figure 12. Total chloride concentration along the depth of three concrete specimens with different aggregate shapes, after4yearsofexposure [32].

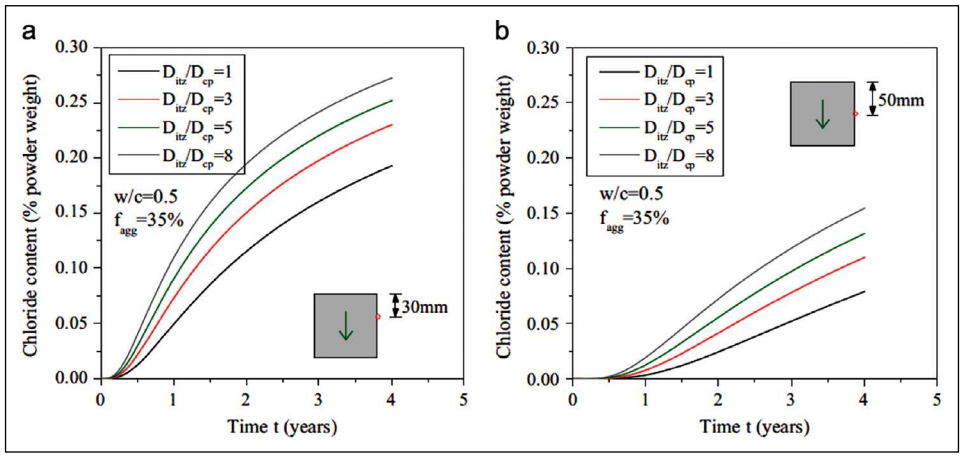

Figure 13. Chloride content-time of the specimen: **(a)** at cover depth=30 mmand **(b)** depth=50mm [32].

2.1.2. Meso-Scale Modeling

Du et al. [32], in their research, develop a heterogeneous model including mortar matrix, aggregate, and ITZ to examine chloride diffusivity of concrete, especially RAC [32]. In the model, aggregates are assumed as an impermeable material and the chloride diffusion occurs through the mortar matrix and ITZs [32]. The diffusivity parameters of components, such as mortar matrix and ITZs, are obtained in the literature, and the model simulated in Abaqus is validated with the test given in the literature [32]. The transient analysis is chosen, and the period is 4 years [32]. 4-node linear heat transfer quadrilateral elements are used for concrete [32]. As a results, it is concluded that three different aggregate shape (squared and circular, elliptical) don't affect the chloride diffusion performances of RAC for the same aggregate volume ratio in concrete (Fig. 12) and, the chloride diffusion increases when ITZs thickness increases due to more porous structure and higher water/cement ratio of ITZ in comparison to the cement paste (Fig. 13) [32].

Kim et al. [33] conduct a series of numerical analysis on porous concrete pile (RAPP) produced with RA and compared the results with the numerical simulation results using Abaqus [33]. RAPP is modeled as a vertical drainage in Ref. [33]. In the modeling part, RAPP and the clay formation are simulated by using the Mohr–Coulomb model and the modified Cam clay model, respectively [33]. For all the components, 4-node bilinear displacement and the pore pressure element (CAX4P) is used [33]. It is stated that RAPP considerably contributes to enriching consolidation with supplying radial drainage [33].

Xiao et al. [34] examine the ITZs effects on stress-strain of RAC. In this paper, RAC is modeled in meso/micro scale in Abaqus (Fig. 14). The plastic-damage constitutive models are used, and the model is simulated to determine mechanical behavior (i.e., compression and tension) [34]. In Explicit step, ABAQUS/explicit quasi-static solver is used [34]. While defining the properties of ITZ and other parts, concrete damaged plasticity is considered and the properties of parts are based on experimental data (i.e., nano-indenta-

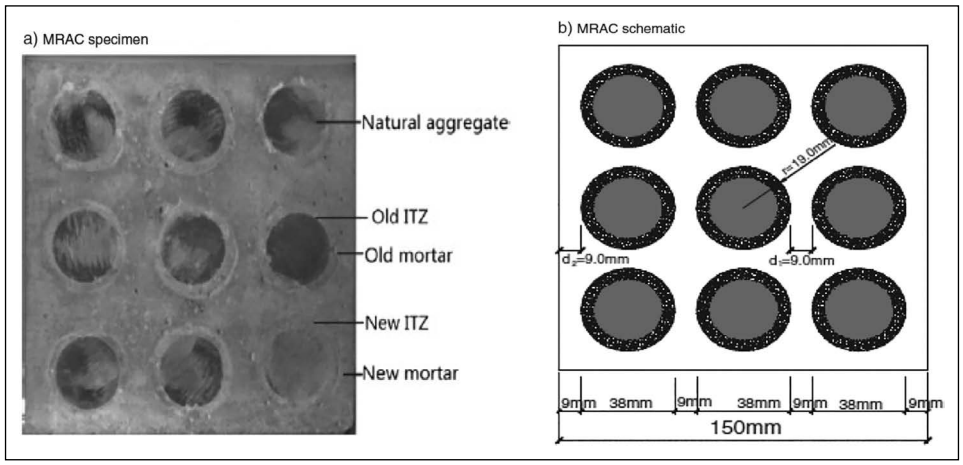

Figure 14. Modeled recycled aggregate concrete (MRAC) [34].

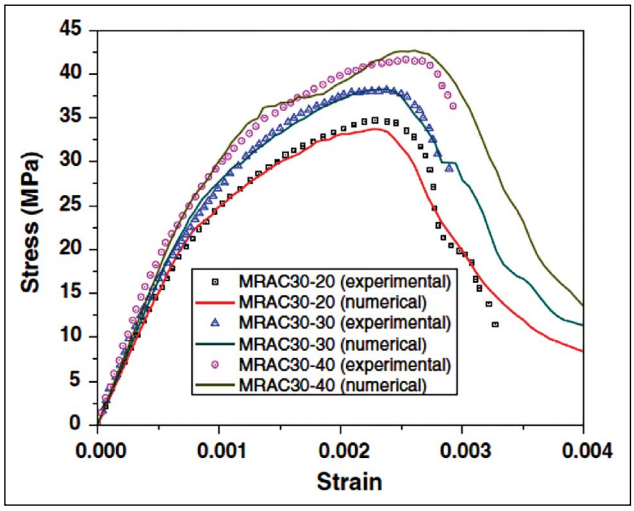

Figure 15. Compressive stress–strain curves with different new mortar matrices [34].

tion tests) [34]. It is concluded that the mortar matrixes and ITZs has a significant role on failure patterns and stress–strain relationship of modeled RAC (MRAC) (Fig. 15) [34].

Xiao et al. [35] propose a model to define the RA effect on chloride diffusion in RAC using Abaqus (Fig. 16). In the simulation part, a five-phase composite for RAC is modeled (Fig. 17) (these phases are old and new ITZs, old and new mortar, and original aggregate) [35]. The transient analysis and the 8-node quadratic heat transfer quadrilateral element are chosen for the model [35]. It is stated that the suggested heterogeneous RAC FE model works well and gives realistic chloride diffusion results [35].

Wang et al. [11] study the influence of old concrete carbonation on ITZ properties of RAC. In this paper, old concretes with various water/binder ratios are considered and modeled and are carbonated [11]. Then, the peak load, the load–displacement curves, and the peak displacement are examined to define the effect of carbonation on modeled RAC [11]. The model is simulated in Abaqus and is verified

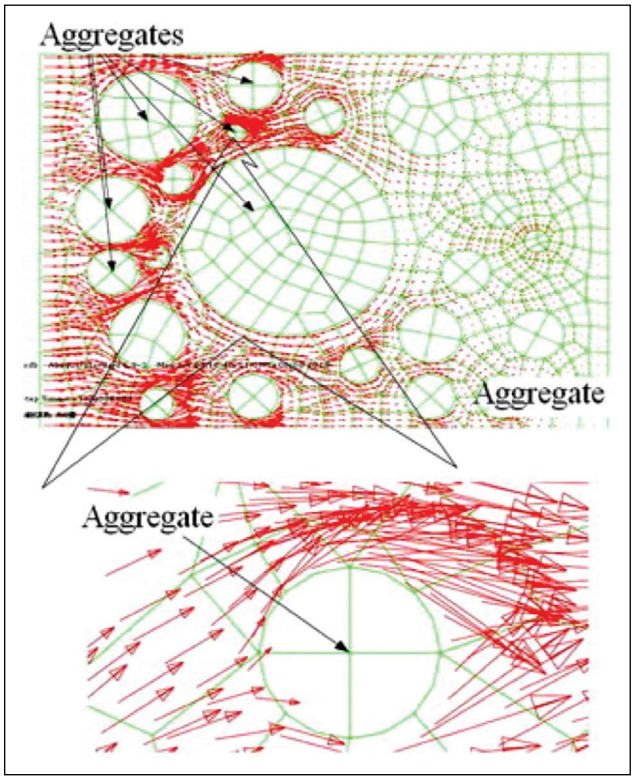

Figure 16. The chloride flow in modeling concrete [35].

with the test data [11]. In the modeling of mortar matrix and ITZ, the constitutive relationship of mortar matrix and ITZ is defined with damage plasticity model in Abaqus [11]. It is stated that ITZ properties have similarity with mortar matrix properties, however elastic modulus, and strength of ITZ are lower than the mortar matrix in the model [11]. On the other hand, in the modeling of natural aggregate (NA), NA is considered and modeled as an isotropic material [11]. In FEA, ABAQUS/explicit solver is used to solve FEM equations [11]. As a results, it is stated that ITZ properties of modeled RAC is considerably related with shape of RA, distribution of old mortar, and carbonation depth [11].

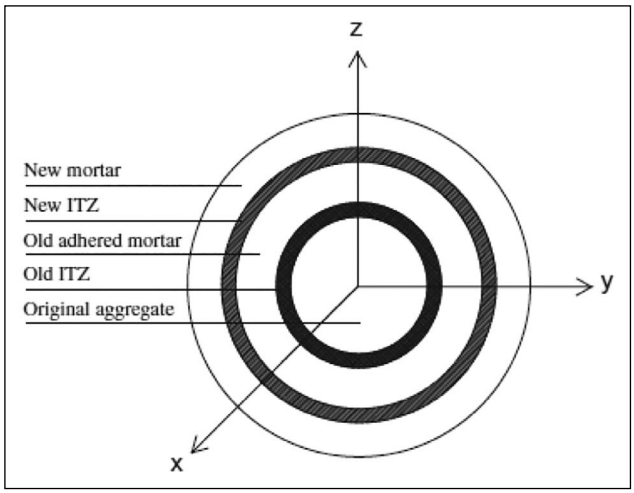

Figure 17. Five-phase composite sphere mode [35].

Ying et al. [10] investigate the effect of RA ratio on chloride diffusion in RAC using Abaqus (Fig. 18). The transient analysis and the 8-node quadratic heat transfer quadrilateral element are selected for FEM [10]. It is concluded that the consistent tendency for compressive strength and chloride migration in modeled RAC is observed and FEA results are verified with test results [10].

Xiao et al. [36] investigate RAC stress distribution while a pressure load is applied to RAC model in Abaqus. In FEA, overall mechanical properties, elastic stress distribution, damage localization and stress concentration are examined (Fig. 19) [36]. The static analysis in Abaqus is adopted to FEM and the linearity in the analysis is considered [36]. In conclusion, it is recommended that ITZ presents a strain softening behavior and the non-linearity in the analysis for ITZ should be considered [36].

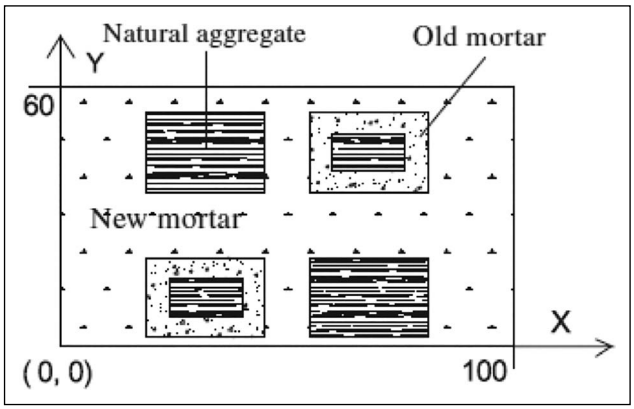

Figure 18. The MRAC containing modeled RA and NA [10].

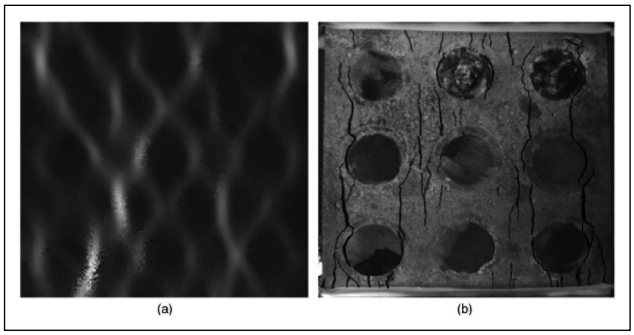

Figure 19. Testing results on the MRAC under uniaxial loading by the digital image correlation: **(a)** horizontal field strain contour map; **(b)** crack pattern [36].

2.1.3. Micro-Scale Modeling

Jeong et al. [37] study on the time-dependent hydration phenomenon chemo-thermal modeling of mortars included RA and NA. In this paper experimental and theoretical

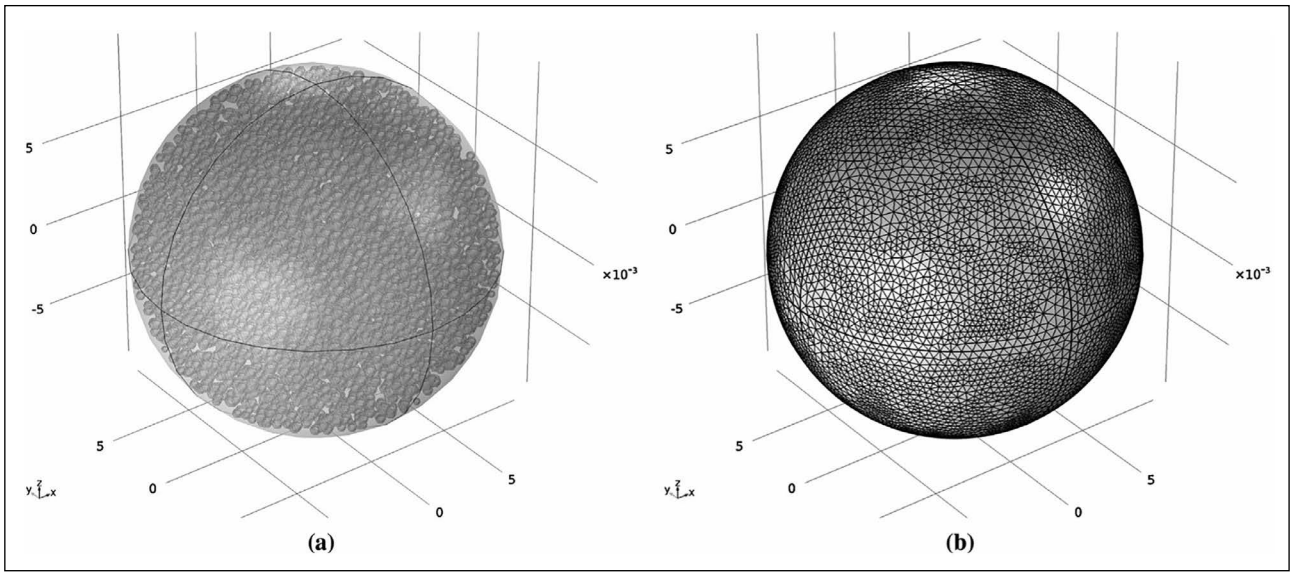

Figure 20. Illustration of geometrical configurations of M2-1 numerical EAG specimens, **(a)** cement matrix including 4149 sand grains and **(b)** mesh density [37].

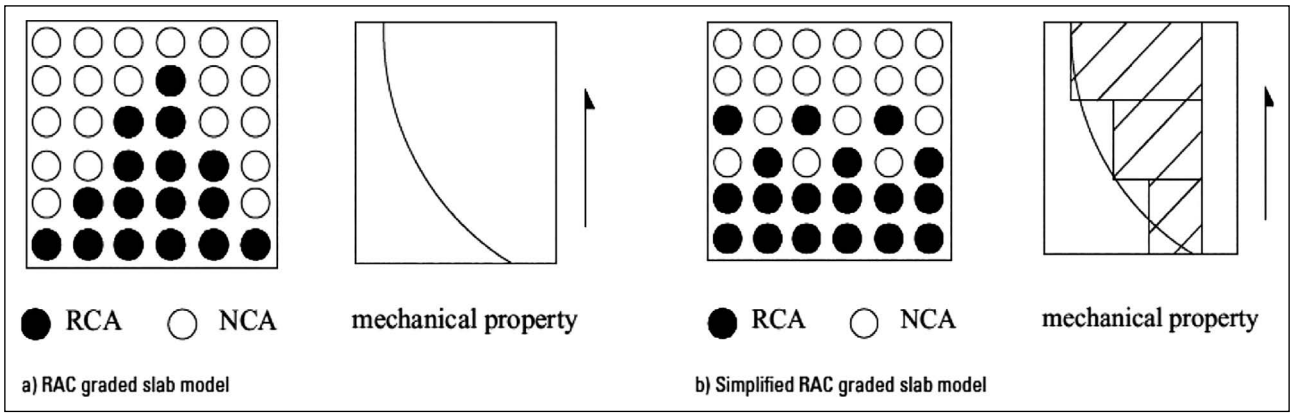

Figure 21. RAC graded slab models [38].

Table 2. Comparisons between ABAQUS simulation and experiment [38]

Slab No.		Yield load (kN)	Ultimate load (kN)	Yield displacement (mm)
5f-1	Test	25.2	31.6	29.2
	ABAQUS	27.5	30.3	16.2
5h	Test	22.0	30.5	28.0
	ABAQUS	26.5	29.8	17.3
5f-2	Test	18.2	29.3	27.7
	ABAQUS	24.4	33.4	13.3
7f-1	Test	27.8	39.6	16.7
	ABAQUS	37.5	41.1	15.6
7h	Test	28.0	39.2	19.9
	ABAQUS	28.3	41.5	14.2
7f-2	Test	26.8	39.8	12.9
	ABAQUS	36.1	43.4	15.3

analysis are conducted and the modified Arrhenius' law and 3D FEA are considered [37]. In the modeling section, the Extracted Aggregate Groups (EAGs) concept is formed and has spherical geometry (Fig. 20) [37]. During the hydration process, the isotropic chemo-thermal features in the calorimeter device is considered [37]. Also, the pseudo-random geometric spherical packing algorithm is considered [37]. In this paper, the grains in the mortar are modeled and formed in Matlab-Comsolcode [37]. In the modeling, it is pointed out that the chemo-thermal modeling is in non-linear transient-state because the chemical reactions of cement paste have the non-linear features [37]. In conclusion, according to a user-written Matlab-Comsolcode FEA and the experimental results, the modified Arrhenius' law is not useful for the recycling mortar hydration modeling [37]. Hence, a revision is need for the modified Arrhenius' law if it is used for the recycling mortar hydration modeling [37].

3. REINFORCED RECYCLED AGGREGATE CONCRETE

It is well-known that the rebar behavior with concrete works together perfectly, and hence many concrete works included rebars and concrete, and investigations on their behavior are implemented around the world. In the literature, in parallel, the reinforced recycled aggregate concrete (RRAC)behavior is examined widely, and especially the comparative studies on RRAC, and reinforced NAC (RNAC) are done. Researchers are generally inspired to determine the properties of RRAC under the static and the dynamic loading conditions to assess the properties of RRAC (i.e., punching). Hence, in this section, the papers on modeling of RRAC are reviewed in two sub-sections consisted of the static and the dynamic loading conditions.

3.1. Modeling of Reinforced Recycled Aggregate Concrete

3.1.1. Behavior Under Static Loading Conditions

Xiao et al. [38] investigate RRAC graded slabs with 0-50-100% RA. The gradation of RA is done in consideration of the stress state in the element (Fig. 21) [38]. In the FEM, the flexural behavior of the slabs, the grading models effect, and the different reinforcement ratios effect are examined in Abaqus [38]. The rebars are embedded in RAC and the bond slip is not considered [38]. The slab model is divided into 3 parts due to the RRAC graded slab modeling method, and the divided parts have different material properties [38]. As a results, it is concluded that RRAC graded slabs presents a good flexural behavior and is feasible to simulate in a FEM (Table 2) [38].

Pacheco et al. [39] study on concrete structures made with RA to analysis the vertical load effect on the slabs. The two-stories concrete structure is designed according to Eurocode 2 and 8 (Fig. 22) [39]. In the modeling section, a 3D concrete structure is modeled using linear FEM in CSI SAP 2000 v.15, and the elasticity modulus of the concretes is predicted by FEM calibration [39].

Francesconi et al. [40] examine the punching shear behavior RRAC slabs with 30-50-80-100% RA. A linear FE slab model is simulated to obtain the prediction of the slab rotation. It is stated that the reinforcement in slab has an important role [40].

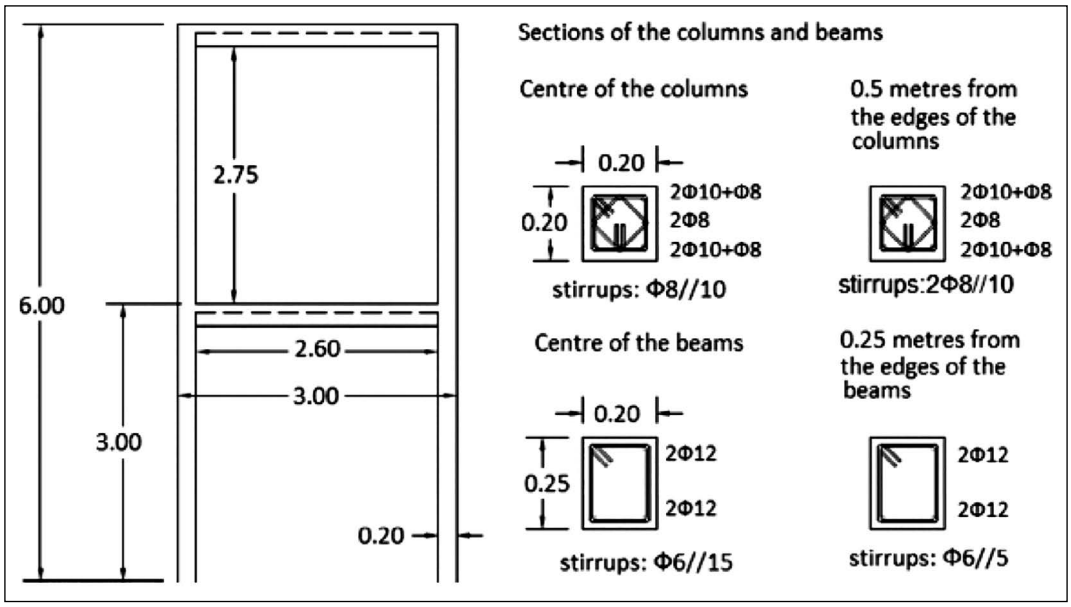

Figure 22. Geometry and reinforcement layout of the test-structures [39].

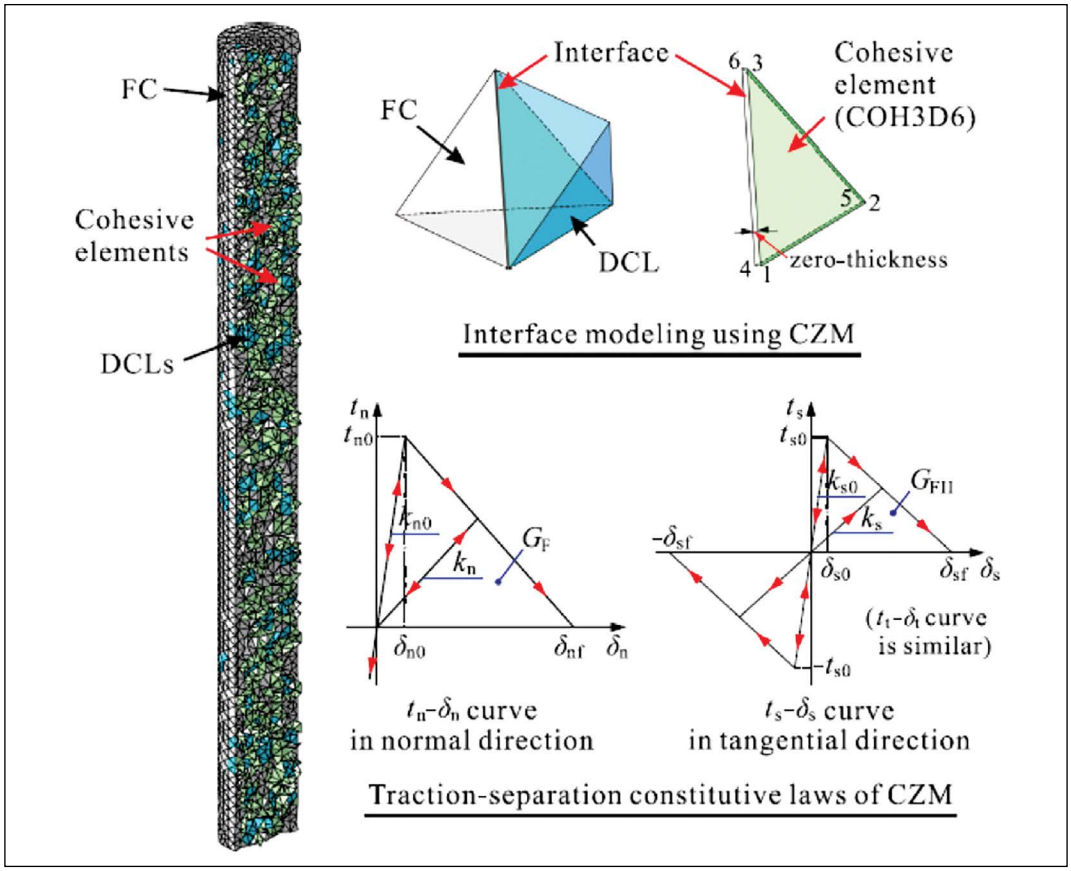

Figure 23. Cohesive zone model (CZM) and its traction-separation constitutive laws [41].

Zhao et al. [41] conduct research on thin-walled circular steel tubular columns and the columns indicate demolished concrete lumps (DCLs) and fresh concrete (FC) [41]. Under consideration of Monte Carlo simulation technique, a non-linear 3D FE model is simulated in Abaqus [41]. In the model DCLs are fully bonded and considered to have a random spatial distribution [41]. Also, the cohesive zone model (CZM) is adopted for the zone between DCLs and FC (Fig. 23) [41]. In

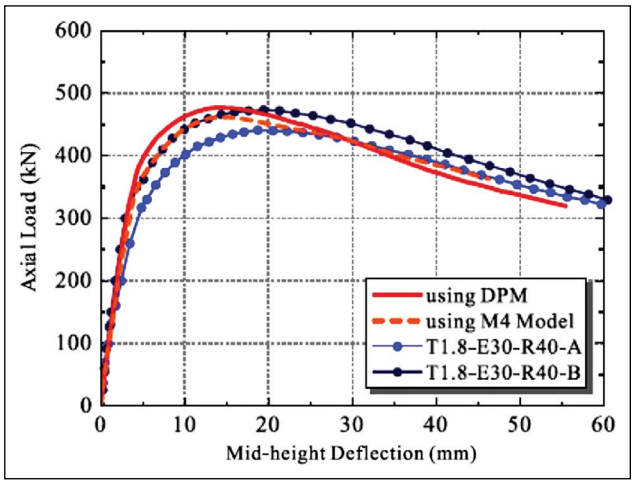

Figure 24. Comparison of simulation results using DPM and M4 model against test results [41].

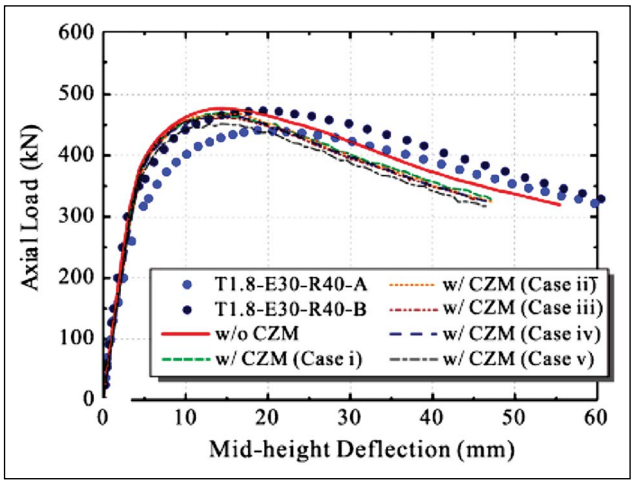

Figure 25. Comparison of simulation results with and without CZM against test results [41].

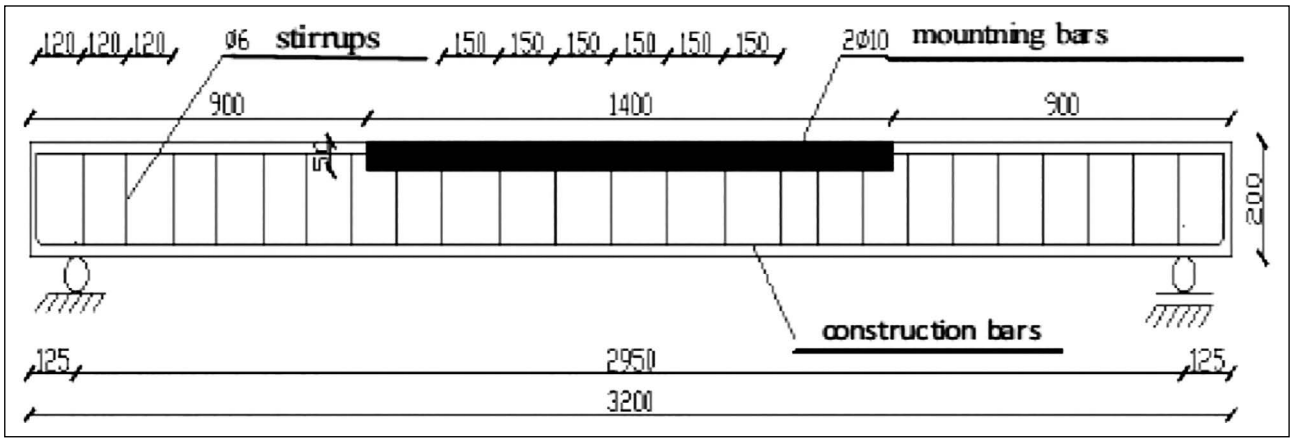

Figure 26. The scheme of innovative full-scale beam made of RAC with the insert made of HSC-HPC [42].

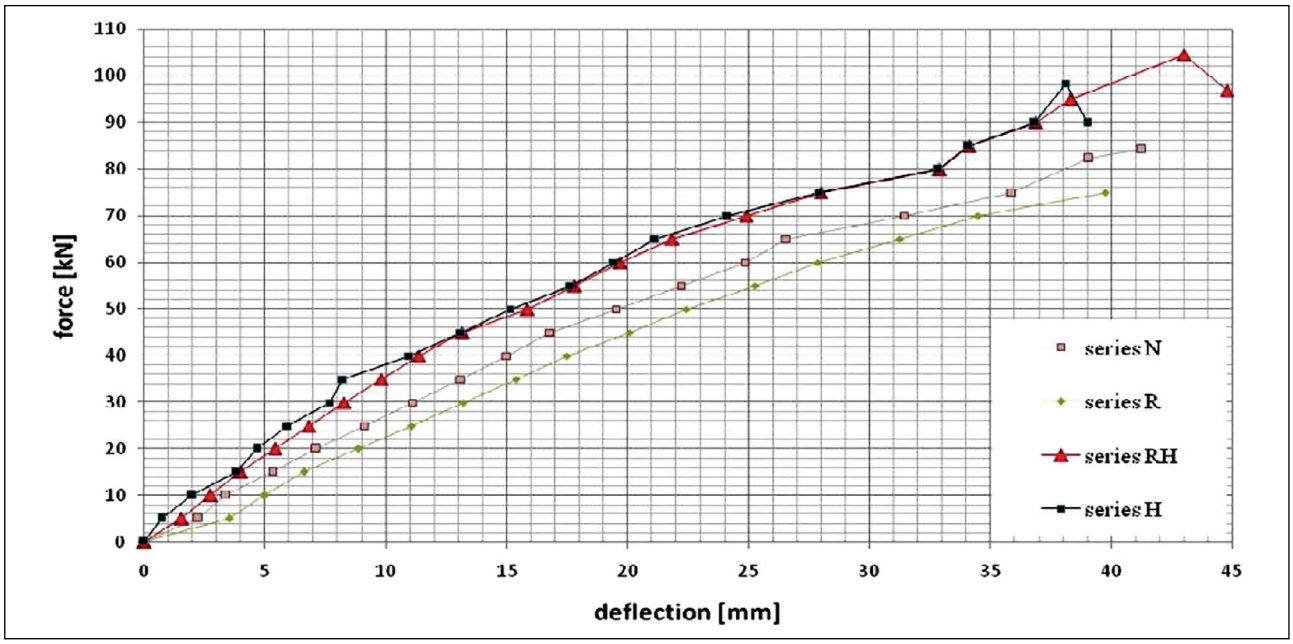

Figure 27. Comparison of average deflections of full-scale beams [42].

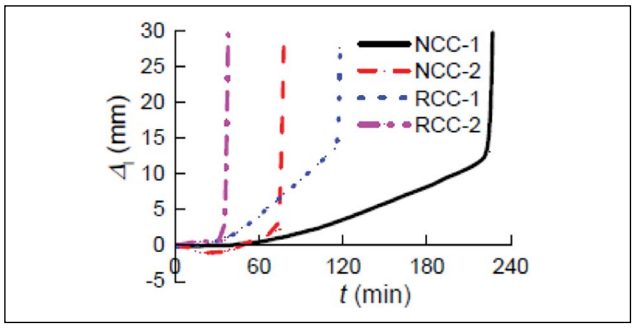

Figure 28. Specimen "vertical displacement to time" curves [43].

this research, the micro-plane model M4 developed by Bazant and based on kinematic constraint, and damaged plasticity model are considered in Abaqus for concrete constitutive modeling to compare the models (Fig. 24) [41]. The models are two inelastic constitutive laws and are well-established in the literature [41]. Then, it is concluded that the columns with DCLs are found suitable in reliance on a strength-reduction factor of 0.9 (Fig. 25) [41].

Lapko and Grygo [42] study on RRAC flexural members which include High Strength Concrete (HSC) - High Performance Concrete (HPC) locally (Fig. 26, 27). In this innovative concept, the non-linear FEMs are simulated in Diana FEA software and a Newton-Raphson algorithm is used in the FEM numerical solutions [42]. Also, the rebars are modeled as REBAR in Diana [42]. It is concluded that the use of HSC-HPC in compression zone of the reinforced beam considerably increase the stiffness and influence the deflections and strains [42].

Dong et al. [43] examine the effects of concrete compressive strength on the fire resistance performance of RRAC columns with C20 and C30 strength classes [43]. While the column is exposed to the fire, a constant axial force is subjected [43]. In the modeling part of the research, the four lateral sides of columns are exposed to the fire [43]. It is concluded that RRAC columns have higher fire resistance than conventional concrete if the columns have same compressive strength (Fig. 28) [43].

3.1.2. Behavior Under Dynamic Loading Conditions

Pacheco et al. [44] study on concrete structures made with RA to analysis the dynamic characterization of full-scale structures. In this paper, the two-stories3D concrete structure designed according to Eurocode 2 and 8is modeled using linear FEM in CSI SAP 2000 v.15, and elasticity modulus and modes of the structures are determined by FEM calibration (Fig. 29–31) [44]. It is concluded that the use of superplasticizers in RAC increase the elasticity modulus and is a good option, and the results of modal damping have high scatter (Fig. 32) [44].

Fu et al. [45] conduct a numeric study on seismic behavior of RRAC beams which is under torsion forces (Fig. 33). The numerical RRAC model is formed in Abaqus (Fig. 34) [45]. In the modeling part, the material behavior is defined in the plastic-damage model in Abaqus, and the stress-strain constitutive relationship of concrete is defined using Sargin model [45]. In the FEM, the rebars are embedded to the concrete and the non-linear analysis is adopted to model [45]. It is stated that the typical torsional failure in RRAC and RNAC beams are found similar [45].

Cao et al. [46] investigate the seismic performance of recycled concrete brick walls (RCBW) and study on the lateral load-displacement relations and the elastic-plastic deformation characteristics of RCBW. In the paper, vertical

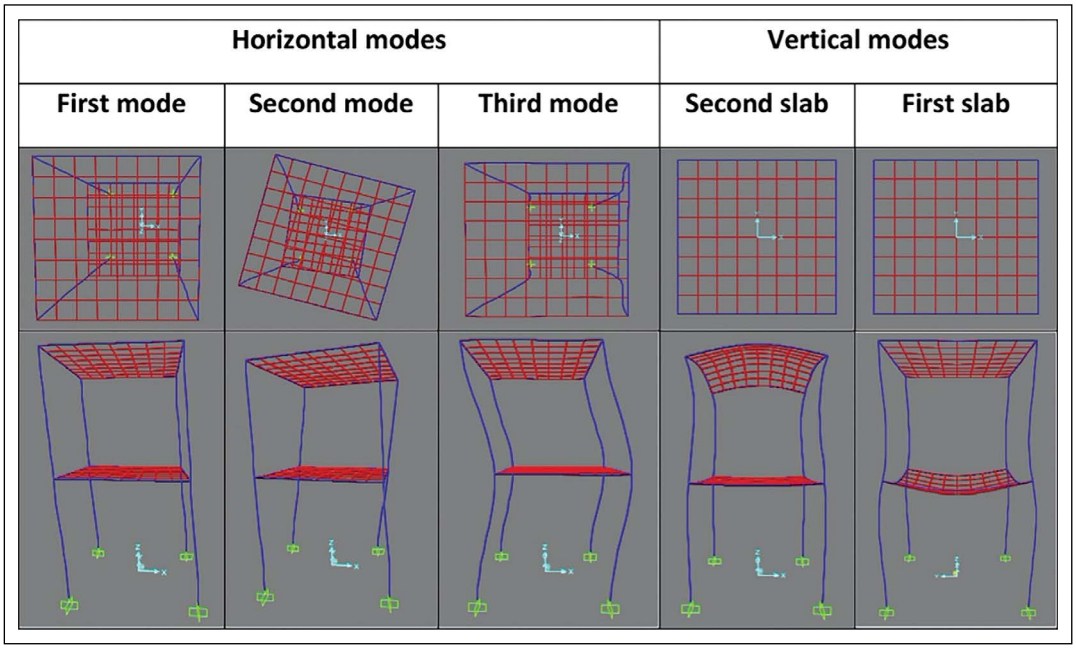

Figure 29. Modal configurations [44].

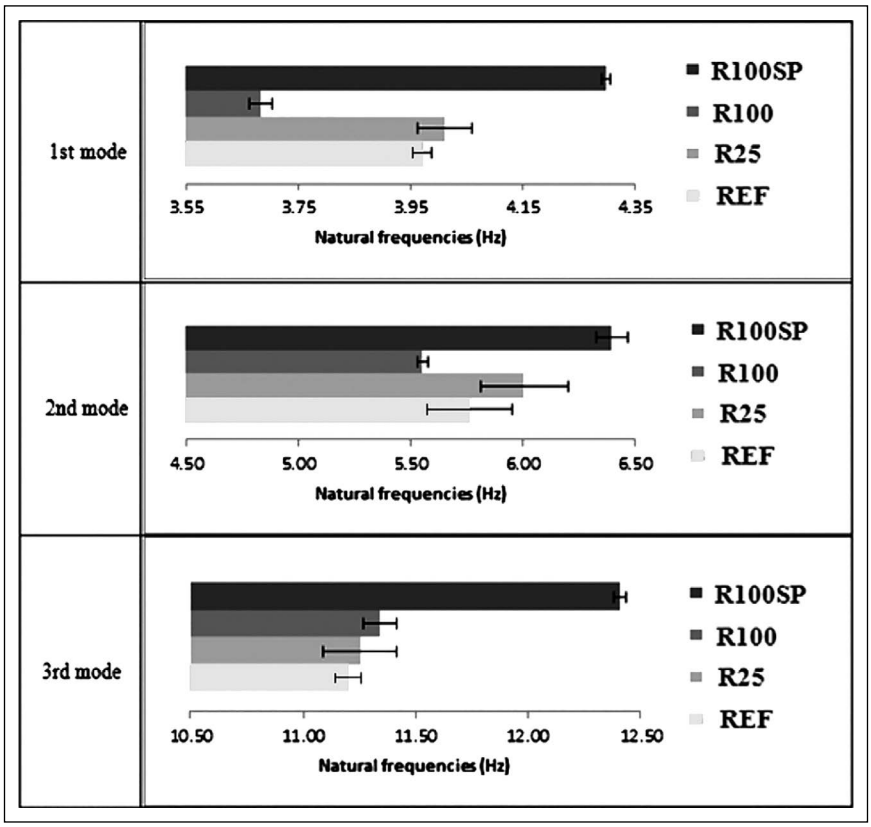

Figure 30. Average horizontal frequencies and confidence intervals (forced vibrations, seismograph) [44].

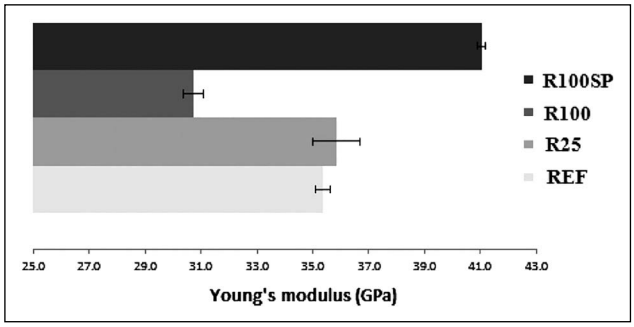

Figure 31. Average elasticity modulus after calibration and confidence intervals (seismograph) [44].

reinforcement is used and embedded in RCBW (Fig. 35), and RCBW FEMs are simulated in Abaqus [46]. The plastic-damage model and the plasticity model in Abaqus are considered for RCBW and the reinforcement of RCBW, respectively [46]. The contact between all the interface models is defined as hard contact and Coulomb friction model is adopted for the contact on the lateral axis [46]. As a results, it is concluded that RCBW with vertical reinforcement may be a good choice for the rural low-rise buildings when the seismic design of the low-rise buildings is considered [46].

Xiao et al. [47] study on the semi-precast column included NA and RA (Fig. 36, 37), and the columns are subjected to the low cyclic horizontal loading. In this paper, the columns are simulated in FEA software ANSYS [47]. In the modeling section, the concrete parameters are defined in the William–Warnke failure criterion and the smeared cracking model, and the double-slash elastic–plastic model is used for rebars [47]. The non-linear FE modeling demonstrates that the semi-precast RRAC and RNAC columns present a similar seismic behavior, and the bearing capacity increases when the core column RAC strength increases [47].

4. SUMMARY

This paper indicates a state-of-the-art review on the related investigations and results on macro-, meso- and micro-scale FE modeling of pure recycled aggregate concrete (RAC) and reinforced RAC (RRAC) under static and dynamic loadings. According to the comments stated above, generally concrete properties are able to be utilized as a non-linear parameter in FEA with various constitutive models (i.e., concrete damaged plasticity and concrete smeared cracking models in Abaqus), and hence this concept ensures to get closer results to reality and to puts out material behavior clearly. This phenomenon is valid for not only pure RAC but also RRAC. On the other hand, many simulation studies are conducted using FEA, some branches of science on pure and reinforced RAC stay short in the literature (i.e., micro-scale behavior of RAC). As a result, the followings can be drawn:

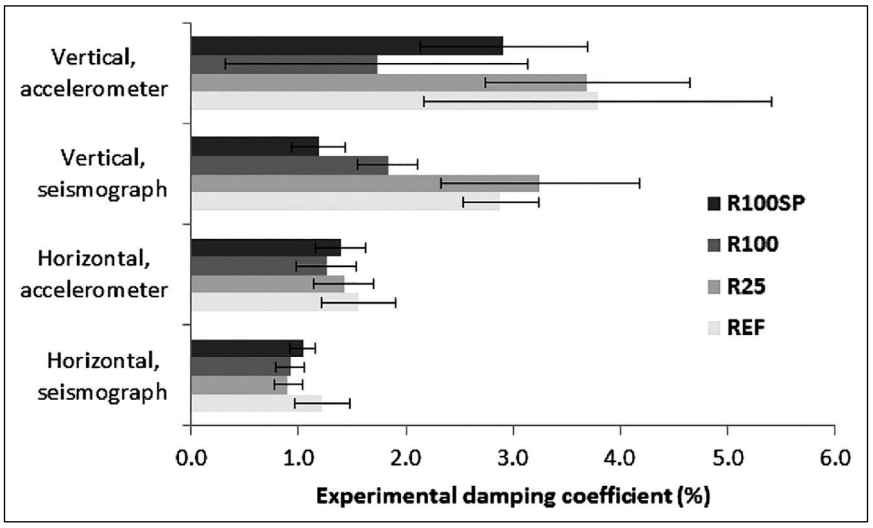

Figure 32. Average damping estimation and confidence intervals [44].

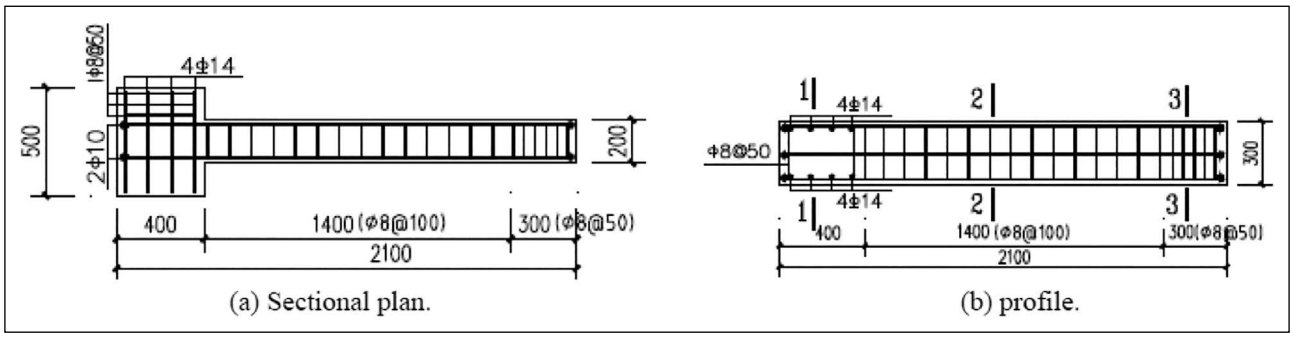

Figure 33. Specimen configuration and reinforcement details [45].

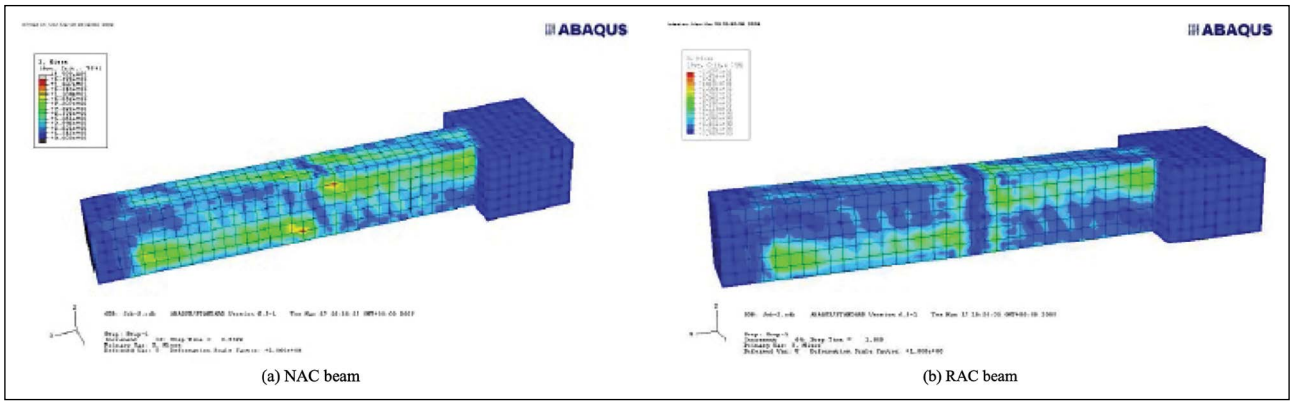

Figure 34. Von Misses stress of the two kinds of specimens [45].

(1) RAC

- It is necessary to determine the micro-scale behavior of RAC and the micro-scale behavior of RAC can be modeled in FEM.
- The harmful environment effects on RAC can be modeled in FEM considering macro-, meso- and micro-scale behavior of RAC (i.e., freeze-thaw and chemical attack effects).
- The properties of RAC and its components (attached old mortar, new and old ITZ etc.) should be determined after a fire effect, a chemical attack, etc. subjected to RAC. Here, the gradient of the properties of RAC and its components under the effects commented before can be determined, and then RAC can be modeled properly in FEM. It is thought that the next features of RAC are substantial as much as the initial features of RAC, especially for the durability properties of RAC.
- The chemical and mineral additions effects on mi-

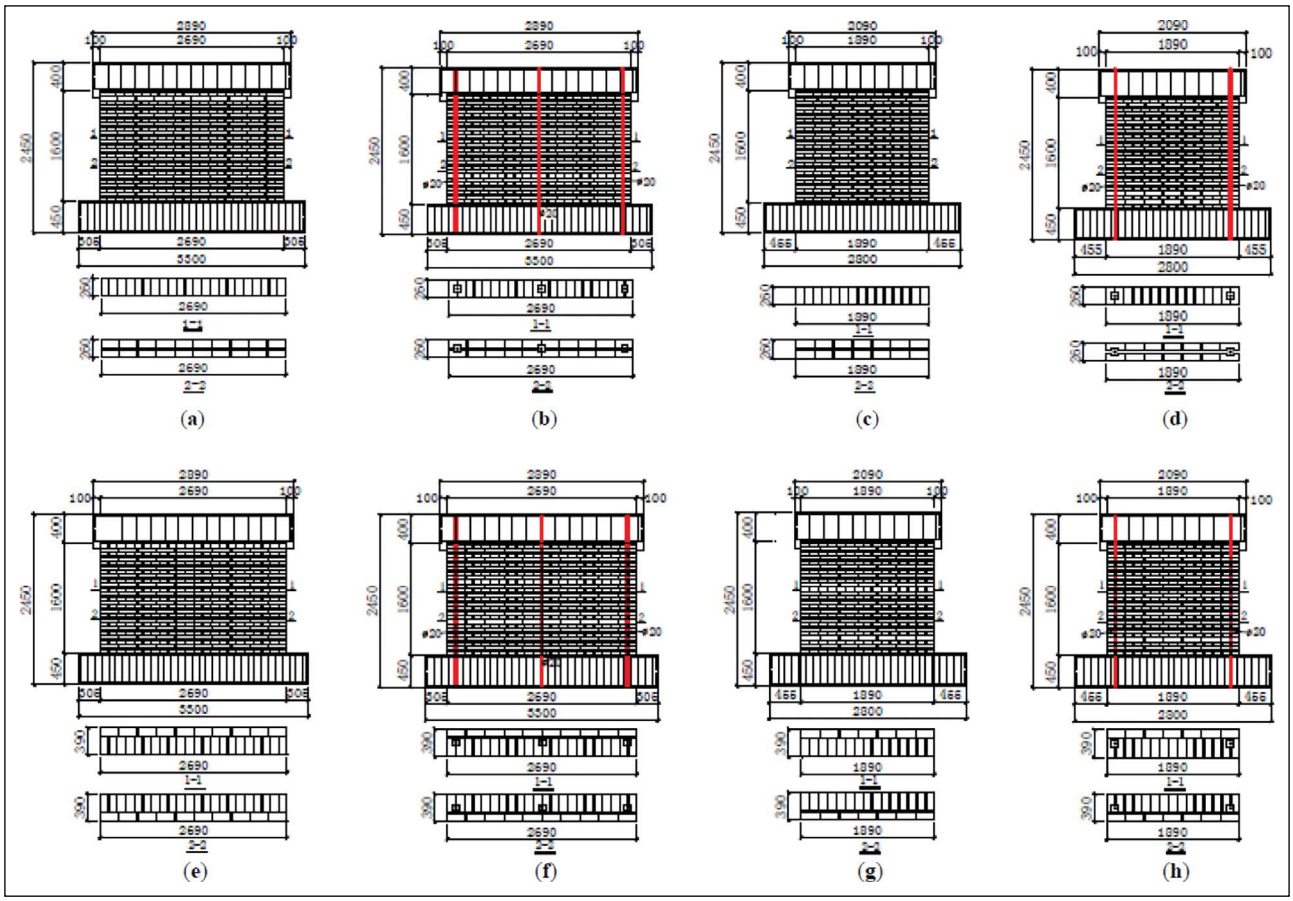

Figure 35. The dimensions and details of all the specimens: **(a)** MWA-1; **(b)** MWB-1; **(c)** MWA-2; **(d)** MWB-2; **(e)** MWA-3; **(f)** MWB-3; **(g)** MWA-4; **(h)** MWB-4. (Unit: millimeter) [46].

cro-scale behavior of RAC can be analyzed and modeled. For instance, the mineral additions improve the quality of mortar due to the formation of additional silicate gels (C-S-H) and this phenomenon can be modeled in micro-scale.

- RAC subjected to the cyclic loading conditions can be examined and RA effect on the macro-, meso- and micro-scale behavior of RAC can be determined. Also, the crack propagation in the RAC mass due to the cyclic loading can be modeled and the effective factors can be examined in FEM.

(2) RRAC

- Under the consideration of RRAC seismic behavior, the factors enhance the RAC structure seismic performance can be determined and modeled in FEM. Especially, starting from element to structure (from micro-scale to macro-scale), the rebar design in cross-sections should be properly considered and then experiments can be conducted to verify the results or both can be done.
- Stirrup effect on RRAC under various loads and moments conditions should be determined and FEM models can simulate the conditions. Hence, it can be seen how the probable situations affect the structural performance.
- The harmful environment effects on RRAC can be modeled in FEM and its effect on structural performance can be determined.
- RRAC subjected to the cyclic loading conditions can be examined and RA effect on the micro-, meso- and macro-behavior of RRAC can be determined. Also, the crack propagation in the RAC mass of RRAC and the interface between the rebars and RAC of RRAC due to the cyclic loading can be modeled and hence, it can be seen how the probable situations affect the structural performance.

DATA AVAILABILITY STATEMENT

The author confirm that the data that supports the findings of this study are available within the article. Raw data that support the finding of this study are available from the corresponding author, upon reasonable request.

CONFLICT OF INTEREST

The author declare that they have no conflict of interest.

FINANCIAL DISCLOSURE

The author declared that this study has received no financial support.

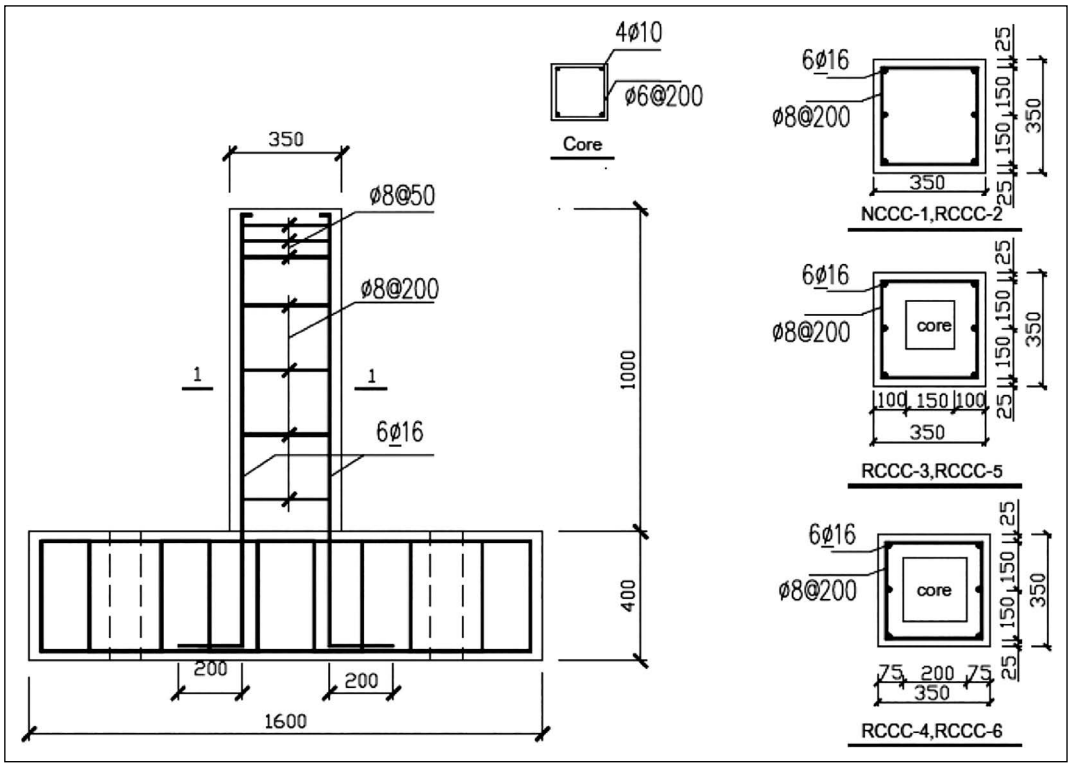

Figure 36. Reinforcement diagram of specimens [47].

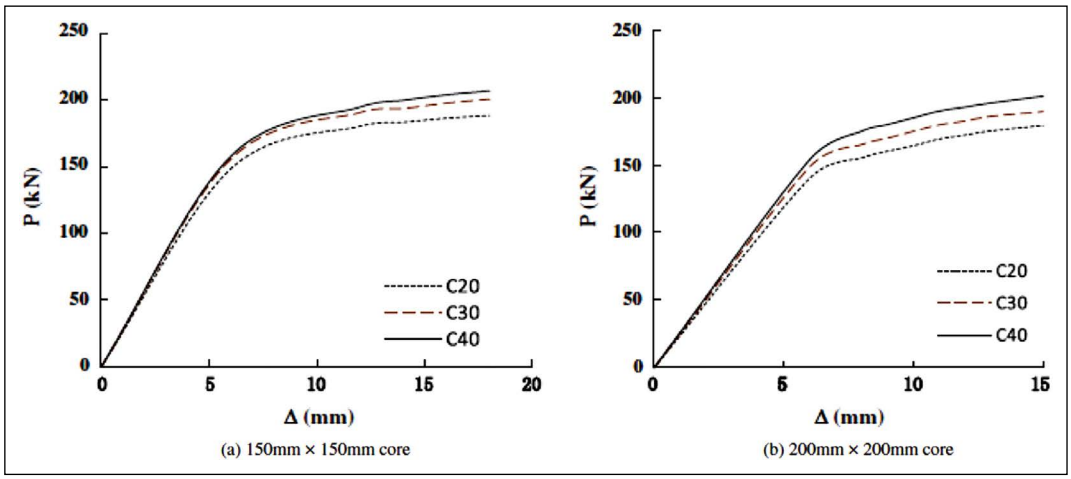

Figure 37. Effect of core compressive strength on the load – deflection (P-Δ) relationship [47].

PEER-REVIEW

Externally peer-reviewed.

REFERENCES

[1] Dilbas, H., Şimşek, M., Çakır, Ö. (2014). An Approach for Construction and Demolition (C&D) Waste Disposal through Concrete Using Silica Fume, in: EurAsia Waste Management Symposium, Istanbul, Turkey.

[2] Xiao, J., Li, W., Fan, Y., Huang, X. (2012). An overview of study on recycled aggregate concrete in China (1996–2011). *Construction and Building Materials*, 31, 364–383. [CrossRef]

[3] European Parlement (2008), Directive 2008/98/EC of The European Parliament and of The Council of 19 November 2008 on Waste and Repealing Certain Directives (text with EEA relevance). Brussels, Belgium.

[4] Dilbas, H. (2014). *An examination on mechanical behaviour of a cantilever beam produced with recycled aggregate concrete* [Unpublished master disser-

tation], Yıldız Technical University.
[5] Dilbas, H., Şimşek, M., Çakır, Ö. (2014). An investigation on mechanical and physical properties of recycled aggregate concrete (RAC) with and without silica fume. *Construction and Building Materials*, 61, 50–59. [CrossRef]
[6] Akça, K., Çakır, Ö., İpek, M. (2015). Properties of polypropylene fiber reinforced concrete using recycled aggregates. *Construction and Building Materials*, 98, 620–630. [CrossRef]
[7] Çakır, Ö. (2014). Experimental analysis of properties of recycled coarse aggregate (RCA) concrete with mineral additives. *Construction and Building Materials*, 68, 17–25. [CrossRef]
[8] Duan, Z.H., Poon, C.S. (2014). Properties of recycled aggregate concrete made with recycled aggregates with different amounts of old adhered mortars. *Materials and Design*, 58, 19–29. [CrossRef]
[9] Gaedicke, C., Roesler, J., Evangelista, F. (2012). Three-dimensional cohesive crack model prediction of the flexural capacity of concrete slabs on soil. 94, 1–12. [CrossRef]
[10] Ying, J., Xiao, J., Tam, V.W.Y. (2013). On the variability of chloride diffusion in modelled recycled aggregate concrete. *Construction and Building Materials*, 41, 732–741. [CrossRef]
[11] Wang, C., Xiao, J., Zhang, G., Li, L. (2016). Interfacial properties of modeled recycled aggregate concrete modified by carbonation. *Construction and Building Materials*, 105, 307–320. [CrossRef]
[12] Xiao, J., Li, W., Poon, C.S (2012). Recent studies on mechanical properties of recycled aggregate concrete in China-a review. *Science China Technological Sciences*, 55, 1463–1480. [CrossRef]
[13] Dilbas, H., Çakır, Ö. (2016). Fracture and Failure of Recycled Aggregate Concrete (RAC)–A Review. *International Journal of Concrete Technology*, 1, 31–48.
[14] Shi, C., Li, Y., Zhang, J., Li, W., Chong, L., Xie, Z. (2015). Performance enhancement of recycled concrete aggregate – A review. Journal of Cleaner Production, 112, 466–472. [CrossRef]
[15] Behera, M., Bhattacharyya, S.K., Minocha, A.K., Deoliya, R., Maiti, S. (2014). Recycled aggregate from C&D waste & its use in concrete - A breakthrough towards sustainability in construction sector: a review. *Construction and Building Materials*, 68, 501–516. [CrossRef]
[16] Hansen, T.C. (1986). Recycled aggregates and recycled aggregate concrete second state-of-the-art report developments 1945-1985. *Materials and Structures*, 19, 201–246. [CrossRef]
[17] Xiao, J.-Zh., Li, J.-B., Zhang, Ch. (2007). On relationships between the mechanical properties of recycled aggregate concrete: An overview. *Materials and Structures*, 39, 655–664. [CrossRef]
[18] Genikomsou, A.S., Polak, M.A. (2015). Finite element analysis of punching shear of concrete slabs using damaged plasticity model in ABAQUS. *Engineering Structures*, 98, 38–48. [CrossRef]
[19] Dilbas, H., Çakir, Ö., Şimşek, M. (2017). Recycled aggregate concretes (RACs) for structural use: an evaluation on elasticity modulus and energy capacities. *International Journal of Civil Engineering*, 15, 247–261. [CrossRef]
[20] Dilbas, H., Çakır, Ö., Şimşek, M. (2015). Kentsel Dönüşüm Sonucu Oluşan Molozların Geri Dönüşümle Betonda Kullanımı – Silis Dumanı Katkılı Geri Kazanılmış Agregalı Betonlar, 9. Ulusal Beton Kongresi, Antalya. pp. 387–398.
[21] Etse, G., Vrech, S.M., Ripani, M. (2016). Constitutive theory for Recycled Aggregate Concretes subjected to high temperature. *Construction and Building Materials*, 111, 43–53. [CrossRef]
[22] Choubey, R.K., Kumar, S., Chakradhara Rao, M. (2016). Modeling of fracture parameters for crack propagation in recycled aggregate concrete. *Construction and Building Materials*, 106, 168–178. [CrossRef]
[23] Musiket, K., Vernerey, F., Xi, Y. (2016). Numeral modeling of fracture failure of recycled aggregate concrete beams under high loading rates. *International Journal of Fracture*, 203, 263–276. [CrossRef]
[24] Ripani, M., Etse, G., Vrech, S. (2017). Recycled aggregate concrete: Localized failure assessment in thermodynamically consistent non-local plasticity framework. *Computers and Structures*, 178, 47–57. [CrossRef]
[25] Ceia, F.M.A.P.M. (2013). *Shear strength in the interface between normal concrete and recycled aggregate concrete* [Unpublished master dissertation], Tecnico Lisboia. [CrossRef]
[26] Vivian, T. Wang. W.Y.Z., Tao, Z. (2014). Behaviour of recycled aggregate concrete filled stainless steel stub columns. *Materials and Structures*, 47, 293–310. [CrossRef]
[27] Yang, Y., Zhang, Z., Fu, F. (2015). Experimental and numerical study on square RACFST members under lateral impact loading. *Journal of Constructional Steel Research*, 111, 43–56. [CrossRef]
[28] Xiao, J., Huang, Y., Yang, J., Zhang, C. (2012). Mechanical properties of confined recycled aggregate concrete under axial compression. *Construction and Building Materials*, 26, 591–603. [CrossRef]
[29] Xiang, X., Cai, C.S., Zhao, R., Peng, H. (2016). Numerical analysis of recycled aggregate concrete-filled steel tube stub columns. *Advances in Structural Engineering*, 19, 717–729. [CrossRef]
[30] Yang, Y., Zhang, L., Dai, X. (2016). Performance of

recycled aggregate concrete- filled square steel tubular columns exposed to fire. *Advances in Structural Engineering*, 20, 1340–1356. [CrossRef]

[31] Geng, Y., Wang, Y., Chen, J. (2016). Time-dependent behaviour of steel tubular columns filled with recycled coarse aggregate concrete. *Journal of Constructional Steel Research*, 122, 455–468. [CrossRef]

[32] Du, X., Jin, L., Ma, G. (2014). A meso-scale numerical method for the simulation of chloride diffusivity in concrete. *Finite Elements in Analysis and Design*, 85, 87–100. [CrossRef]

[33] Kim, S., Lee, D., Lee, J., You, S.-K., Choi, H. (2012). Application of recycled aggregate porous concrete pile (RAPP) to improve soft ground. *Journal of Material Cycles and Waste Management*, 14, 360–370. [CrossRef]

[34] Xiao, J., Li, W., Corr, D.J., Shah, S.P. Effects of interfacial transition zones on the stress–strain behavior of modeled recycled aggregate concrete. *Cement and Concrete Research*, 52, 82–99. [CrossRef]

[35] Xiao, J., Ying, J., Shen, L. (2012). FEM simulation of chloride diffusion in modeled recycled aggregate concrete. *Construction and Building Materials*, 29, 12–23. [CrossRef]

[36] Xiao, J., Li, W., Asce, S.M., Corr, D.J., Shah, S.P., Asce, M. (2013). Simulation study on the stress distribution in modeled recycled aggregate concrete under uniaxial compression. *Journal of Materials in Civil Engineering*, 25, 504–518. [CrossRef]

[37] Jeong, J., Ramézani, H., Leklou, N. (2016). Why does the modified Arrhenius' law fail to describe the hydration modeling of recycled aggregate? *Thermochimica Acta*, 626, 13–30. [CrossRef]

[38] Xiao, J., Sun, C., Jiang, X. (2015). Flexural behaviour of recycled aggregate concrete graded slabs. *Structural Concrete*, 16, 249–261. [CrossRef]

[39] Pacheco, J., De Brito, J., Ferreira, J., Soares, D. (2015). Flexural load tests of full-scale recycled aggregates concrete structures. *Construction and Building Materials*, 101, 65–71. [CrossRef]

[40] Francesconi, L., Pani, L., Stochino, F. Punching shear strength of reinforced recycled concrete slabs. *Construction and Building Materials*, 127, 248–263. [CrossRef]

[41] Zhao, X., Wu, B., Wang, L. (2016). Structural response of thin-walled circular steel tubular columns filled with demolished concrete lumps and fresh concrete. *Construction and Building Materials*, 129 216–242. [CrossRef]

[42] Lapko, A., Grygo, R. (2013). Studies of RC beams made of recycling aggregate concrete strengthened with the HSC-HPC inclusions. *Procedia Engineering*, 57, 678–686. [CrossRef]

[43] Dong, H., Cao, W., Bian, J., Zhang, J. (2014). The fire resistance performance of recycled aggregate concrete columns with different concrete compressive strengths. *Materials*, 7, 7843–7860. [CrossRef]

[44] De Brito, J., Soares, D. (2017). Dynamic characterization of full-scale structures made with recycled coarse aggregates. *Journal of Cleaner Production*, 142, 4195–4205. [CrossRef]

[45] Fu, J., Liu, B., Ma, J., Zhou, H. (2015). Experimental study on seismic behavior of recycled aggregate concrete torsion beams with Abaqus. *Advanced Materials Research*, 1079, 220–225. [CrossRef]

[46] Cao, W., Zhang, Y., Dong, H., Zhou, Z., Qiao, Q. (2014). Experimental Study on the seismic performance of recycled concrete brick walls embedded with vertical reinforcement. *Materials*, 7, 5934–5958. [CrossRef]

[47] Xiao, J., Huang, X., Shen, L. (2012). Seismic behavior of semi-precast column with recycled aggregate concrete. *Construction and Building Materials*, 35, 988–1001. [CrossRef]